Physics Letters A 384 (2020) 126178

Contents lists available at ScienceDirect

Physics Letters A

www.elsevier.com/locate/pla

Lump-type solutions, rogue wave type solutions and periodic lump-stripe interaction phenomena to a $(3+1)$-dimensional generalized breaking soliton equation

Litao Gai [a,g,*], Wen-Xiu Ma [b,c,d,e,f,**], Mingchu Li [g]

[a] School of Mathematical Sciences, Dalian University of Technology, Dalian, 116024, Liaoning, China
[b] Department of Mathematics, Zhejiang Normal University, Jinhua, 321004, Zhejiang, China
[c] Department of Mathematics and Statistics, University of South Florida, Tampa, FL 33620-5700, USA
[d] School of Mathematics, South China University of Technology, Guangzhou, 510640, Guangdong, China
[e] College of Mathematics and Systems Science, Shandong University of Science and Technology, Qingdao, 266590, Shandong, China
[f] Department of Mathematical Sciences, North-West University, Mafikeng Campus, Private Bag X2046, Mmabatho 2735, South Africa
[g] School of Software, Dalian University of Technology, Dalian, 116620, Liaoning, China

ARTICLE INFO

Article history:
Received 16 November 2019
Received in revised form 23 November 2019
Accepted 25 November 2019
Available online 29 November 2019
Communicated by B. Malomed

Keywords:
$(3+1)$-dimensional GBS equation
Bilinear form
Lump-type solution
Rogue wave type solution
Breather lump wave solution
Periodic lump-stripe soliton

ABSTRACT

In this paper, we present a bilinear form for an extended $(2+1)$-dimensional generalized breaking soliton equation, namely, a $(3+1)$-dimensional generalized breaking soliton (GBS) equation, through using the Hirota direct method. Abundant lump-type solutions, rogue wave type solutions, breather lump wave solutions and interaction solutions are constructed, based on the Hirota bilinear form. Particularly, we generate a type of new interaction solutions in terms of a new combination of quadratic function, trigonometric function and exponential function, namely, a kind of periodic lump-stripe solitons, which is a sort of mixed type solutions of periodic lump-type solitons and stripe solitons. We show that the periodic lump-type solitons will be swallowed by the stripe solitons after they collide. Finally, dynamics characteristics and evolution behaviors are exhibited for the obtained solution waves through particular plots with proper choices of different values for the parameters.

1. Introduction

Researchers usually explore important physical phenomena such as wave physical structures and dynamical behaviors through analytic solutions of nonlinear PDEs. The Hirota bilinear method has been widely and successfully used to solve nonlinear PDEs and obtain their lump solutions [1–8], multiple soliton solutions [9–12], multi-lump solutions [13–15], interaction solutions [6,7,16–19], rogue wave solutions [20], and so on. And other constructing methods [21–25]. Recently, several persons work out a few of new solutions for the following $(2+1)$-dimensional generalized breaking soliton equation [26,27]

$$\begin{aligned}&u_t+\alpha u_{xxx}+\beta u_{xxy}+\gamma uu_x+\lambda uu_y+\delta u_x v=0,\\&u_y=v_x.\end{aligned}\tag{1}$$

Eq. (1) is initially proposed to describe the interaction of Riemann wave propagation along the y-axis and wave propagation along the x-axis, where $u=u(x,y,z,t)$ and $v=v(x,y,z,t)$ represent the physical quantities to two wave propagation directions, respectively, and α, β, γ, λ and δ are the relevant parameters [26]. Ma and Li get the mixed soliton and rogue wave solutions of Eq. (1) with the aid of bilinear form [26]. Soliton solutions, homoclinic breather waves and rogue waves of Eq. (1) are obtained by using the Hirota bilinear method [27]. Multi-soliton solutions; and periodic type solutions and cross-kink wave solutions of the reduced Eq. (1) are obtained with the help of the Hirota bilinear method [28,29].

In this work, we will introduce a $(3+1)$-dimensional GBS equation based on Eq. (1), which can describe interaction phenomena along with three space directions in nonlinear media:

$$\begin{aligned}&\omega_t+\alpha u_{xxx}+\beta u_{xxy}+\gamma uu_x+\lambda uu_y+\delta u_x v=0,\\&\omega_x=u_x+u_y+u_z,\quad u_y=v_x,\end{aligned}\tag{2}$$

* Corresponding author at: School of Mathematical Sciences, Dalian University of Technology, Dalian, 116024, Liaoning, China.
** Corresponding author at: Department of Mathematics and Statistics, University of South Florida, Tampa, FL 33620-5700, USA.
E-mail addresses: gltpis8888@mail.dlut.edu.cn (Litao Gai), mawx@cas.usf.edu (Wen-Xiu Ma).

https://doi.org/10.1016/j.physleta.2019.126178
0375-9601/

where $\omega=\omega(x,y,z,t)$ is a real function of x, y, z and t. Similarly, Eq. (2) expands the space dimension of Eq. (1) into three, i.e. adding the wave propagation along the z-axis. We have acquired new lump-type solutions, rogue wave type solutions, breather lump wave solutions and periodic lump-stripe interaction phenomena for the $(3+1)$-dimensional GBS equation (2), by utilizing the Hirota bilinear method. We also show the corresponding dynamic and evolution behaviors for those solutions by plotting with suitable special parameters. These results have not been calculated by others before. Hence, we obtained abundant of new solutions by comparison with the references [26–29].

The rest of the paper is organized as follows. In section 2, we present a bilinear form and lump-type solutions for Eq. (2). In section 3, we get rogue wave type solutions. In section 4 and section 5, we construct breather lump wave solutions and periodic lump-stripe solitons for Eq. (2), respectively. Finally, we give some discussions and concluding remarks in section 6.

2. Bilinear form and lump-type solutions

In this paper, we select the following parameters:

$$\lambda=\delta=3\beta,\quad \gamma=6\alpha, \tag{3}$$

and then Eq. (2) can be written as

$$\partial_x{}^{-1}(u_{xt}+u_{yt}+u_{zt})+\alpha u_{xxx}+\beta u_{xxy}+6\alpha uu_x \\ +3\beta uu_y+3\beta u_x\partial_x{}^{-1}u_y=0. \tag{4}$$

2.1. Bilinear form

To obtain a bilinear form of Eq. (4), we consider the following second-order logarithmic derivative transformation

$$u=\psi_x=2(\ln f)_{xx},\quad v=\psi_y=2(\ln f)_{xy}, \tag{5}$$

where $\psi=\mu_x=2(\ln f)_x$, f, ψ and μ are real functions of x, y, z and t. Substituting $u=\psi_x$ into (4), one can obtain the following equation:

$$\psi_{xt}+\psi_{yt}+\psi_{zt}+\alpha\psi_{xxxx}+\beta\psi_{xxxy} \\ +6\alpha\psi_x\psi_{xx}+3\beta(\psi_x\psi_y)_x=0, \tag{6}$$

substituting $\psi=\mu_x$ into Eq. (6), and integrate once with respect to x, namely

$$\mu_{xt}+\mu_{yt}+\mu_{zt}+\alpha\mu_{xxxx}+\beta\mu_{xxxy} \\ +3\alpha\mu_{xx}{}^2+3\beta\mu_{xx}\mu_{xy}=0, \tag{7}$$

by setting $\mu=2\ln f$, then, we see that Eq. (2) is reduced into the following bilinear equation

$$\alpha ff_{xxxx}-4\alpha f_xf_{xxx}+3\alpha f_{xx}{}^2+\beta ff_{xxxy}-\beta f_{xxx}f_y-3\beta f_xf_{xxy} \\ +3\beta f_{xx}f_{xy}+ff_{xt}-f_xf_t+ff_{yt}-f_yf_t+ff_{zt}-f_zf_t=0, \tag{8}$$

and Eq. (2) can be written in terms of P-polynomial [28]

$$P_{xt}+P_{yt}+P_{zt}+\alpha P_{4x}+\beta P_{3x,y}=0. \tag{9}$$

Under the above constraints, Eq. (9) has the Hirota bilinear form

$$\left(D_xD_t+D_yD_t+D_zD_t+\alpha D_x^4+\beta D_x^3D_y\right)f\cdot f=0, \tag{10}$$

where $D_x^4, D_x^3D_y, D_xD_t, D_yD_t$ and D_zD_t are all bilinear operators [30], meet by

$$D_x^KD_y^LD_z^ND_t^M(f\cdot g) \\ =\left(\frac{\partial}{\partial x}-\frac{\partial}{\partial x'}\right)^K\left(\frac{\partial}{\partial y}-\frac{\partial}{\partial y'}\right)^L\left(\frac{\partial}{\partial z}-\frac{\partial}{\partial z'}\right)^N \\ \times\left(\frac{\partial}{\partial t}-\frac{\partial}{\partial t'}\right)^M f(x,y,z,t)g\left(x',y',z',t'\right)\Big|_{x'=x,y'=y,z'=z,t'=t}.$$

2.2. Lump-type solutions

To obtain lump-type solutions of Eq. (2), let f be a quadratic function solution as follows [1–7]

$$f=\zeta_1{}^2+\zeta_2{}^2+g_0, \\ \zeta_i=a_ix+b_iy+c_iz+d_it+h_i,\ i=1,2, \tag{11}$$

where $g_0>0$, and $a_i,b_i,c_i,d_i,h_i(i=1,2)$ are real constants to be calculated. Substituting (11) into bilinear Eq. (10), we reach a set of algebraic equations, and then we can derive $a_i,b_i,c_i,d_i,h_i(i=1,2)$ with the aid of Maple software, which can be classified into the following cases.

Case 1.

$$a_i=a_i(i=1,2),\ b_1=-\frac{\alpha a_1{}^2+\beta a_2b_2+\alpha a_2{}^2}{\beta a_1}, \\ c_1=-\frac{\beta a_1{}^2-\beta a_2b_2-\alpha a_1{}^2-\alpha a_2{}^2}{\beta a_1}, \\ d_i=d_i(i=1,2),\ h_i=h_i(i=1,2),\ b_2=b_2, \\ c_2=-a_2-b_2,\ g_0=g_0,\ \beta=\beta,\ \alpha=\alpha. \tag{12}$$

Case 2.

$$a_1=0,\ c_1=0,\ b_1=0, \\ d_i=d_i(i=1,2),\ a_2=-b_2-c_2,\ b_2=b_2, \\ c_2=c_2,\ h_i=h_i(i=1,2),\ g_0=g_0,\ \beta=\frac{\alpha(b_2+c_2)}{b_2},\ \alpha=\alpha. \tag{13}$$

Case 3.

$$a_1=0,\ b_1=-c_1,\ c_1=c_1, \\ d_i=d_i(i=1,2),\ a_2=-\frac{\beta b_2}{\alpha}, \\ b_2=b_2,\ c_2=\frac{(\beta-\alpha)b_2}{\alpha},\ h_i=h_i(i=1,2), \\ g_0=g_0,\ \beta=\beta,\ \alpha=\alpha. \tag{14}$$

Eqs. (12)∼(14) generate three types of quadratic function solutions $f_i(i=1,2,3)$, defined by (11), to the bilinear Eq. (10); and further the resulting quadratic function solutions present three types of lump-type solutions $u_i(i=1,2,3)$ to Eq. (2), under the transformation $u=2(\ln f)_{xx}$; and three types of lump-type solutions $v_i(i=1,2,3)$ to Eq. (2), under the transformation $v=2(\ln f)_{xy}$. Such as in Case 1, we have

$$f=\Bigg(a_1x-\frac{\alpha a_1{}^2+\beta a_2b_2+\alpha a_2{}^2}{\beta a_1}y \\ -\frac{\beta a_1{}^2-\beta a_2b_2-\alpha a_1{}^2-\alpha a_2{}^2}{\beta a_1}z+d_1t+h_1\Bigg)^2 \\ +(a_2x+b_2y-(a_2+b_2)z+d_2t+h_2)^2+g_0, \tag{15}$$

and

$$u_1=\frac{4\left(-2a_1{}^2\zeta_1{}^2-4a_1a_2\zeta_1\zeta_2-2a_2{}^2\zeta_2{}^2+a_1{}^2f+a_2{}^2f\right)}{f^2}, \tag{16}$$

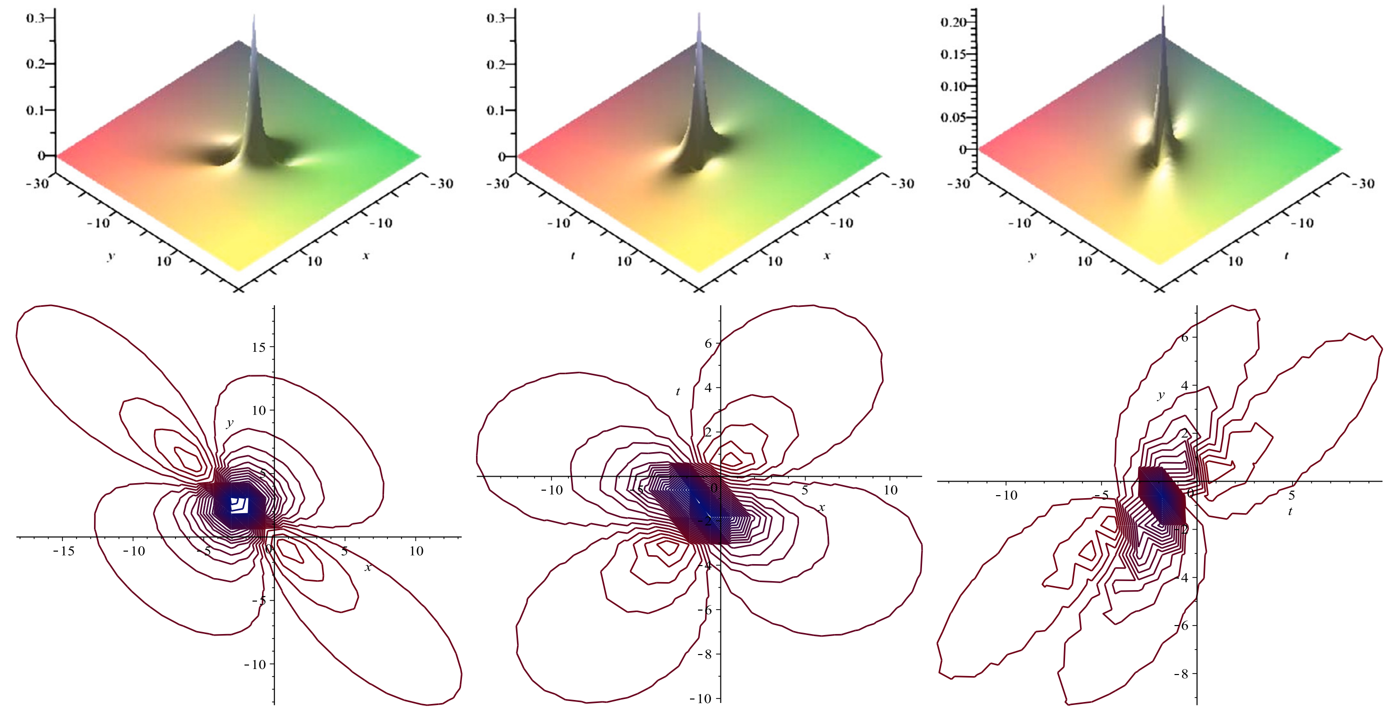

(I) (II) (III)

Fig. 1. The 3-D plots (top) and contour plots (bottom) of u_1 via Eq. (16) at three coordinates: (I) the x_y_u-coordinate by $z=-x$, $t=0$; (II) the x_t_u-coordinate by $z=-x$, $y=0$; (III) the t_y_u-coordinate by $z=-y$, $x=0$; with $a_1=0.2$, $d_1=1$, $h_1=1$, $a_2=0.2$, $b_2=0.2$, $d_2=0.2$, $h_2=1$, $g_0=1$, $\alpha=2$, $\beta=2$.

$$
\begin{aligned}
v_1 = \frac{-4}{\beta a_1 f^2}&(2\beta {a_1}^2 b_2\zeta_1\zeta_2 - 2\beta a_1 a_2 b_2 {\zeta_1}^2 \\
&+ 2\beta a_1 a_2 b_2 {\zeta_2}^2 - 2\beta {a_2}^2 b_2 \zeta_1\zeta_2 \\
&- 2\alpha {a_1}^3 {\zeta_1}^2 - 2\alpha {a_1}^2 a_2\zeta_1\zeta_2 - 2\alpha a_1 {a_2}^2 {\zeta_1}^2 \\
&- 2\alpha {a_2}^3\zeta_1\zeta_2 + \alpha {a_1}^3 f + \alpha a_1 {a_2}^2 f),
\end{aligned} \tag{17}
$$

where $a_1\beta \neq 0$, and the functions ζ_1 and ζ_2 are given as follows:

$$
\begin{aligned}
\zeta_1 &= a_1 x - \frac{\alpha {a_1}^2 + \beta a_2 b_2 + \alpha {a_2}^2}{\beta a_1} y \\
&\quad - \frac{\beta {a_1}^2 - \beta a_2 b_2 - \alpha {a_1}^2 - \alpha {a_2}^2}{\beta a_1} z + d_1 t + h_1, \\
\zeta_2 &= a_2 x + b_2 y - (a_2 + b_2) z + d_2 t + h_2.
\end{aligned} \tag{18}
$$

For lump-type solutions f must be positive, u and v were localized in all directions in the space, so we select $g_0 > 0$. We find that at any given time t, the lump-type solutions $u_i (i=1,2,3) \to 0$ and $v_i (i=1,2,3) \to 0$, if the corresponding sum of squares ${\zeta_1}^2 + {\zeta_2}^2 \to \infty$.

Fig. 1 and Fig. 2 show the 3-D plots and contour plots, which exhibit dynamics properties by choosing appropriate values of these parameters in Eq. (16) and Eq. (17).

3. Rogue wave type solutions

In this section, we will generate rogue wave type solutions to Eq. (2). According to Eq. (10), we search for new type rogue waves of the $(3+1)$-dimensional GBS equation by taking the form [31]

$$
\begin{aligned}
f &= {\zeta_1}^2 + k_1 e^{\zeta_2} + k_2 e^{-\zeta_2} + g_0, \\
\zeta_i &= a_i x + b_i y + c_i z + d_i t + h_i,\ i = 1, 2,
\end{aligned} \tag{19}
$$

where $g_0 > 0$, and $a_i, b_i, c_i, d_i, h_i (i=1,2)$ and $k_i (i=1,2)$ are real constants to be calculated. Substituting (19) into bilinear Eq. (10), we reach a set of algebraic equations, and then we can derive $a_i, b_i, c_i, d_i, h_i (i=1,2)$ and $k_i (i=1,2)$ with the aid of Maple, which can be classified into the following cases.

$$
\begin{aligned}
&a_1 = 0, b_1 = b_1, c_1 = -b_1, d_1 = d_1, h_1 = h_1, a_2 = a_2, \\
&b_2 = -\frac{\beta b_1 {a_2}^3 + d_1 a_2 + d_1 c_2}{d_1}, c_2 = c_2, d_2 = 0, h_2 = h_2, \\
&g_0 = g_0, k_1 = k_1, \beta = \beta, k_2 = k_2, \\
&\alpha = \frac{\beta(\beta b_1 {a_2}^3 + d_1 a_2 + d_1 c_2)}{d_1 a_2},
\end{aligned} \tag{20}
$$

where $d_1 a_2 \neq 0$. Through the transformation Eq. (5), we get the following solutions to Eq. (2)

$$
\begin{aligned}
f = &(b_1 y - b_1 z + d_1 t + h_1)^2 + k_1 e^{(a_2 x - \frac{\beta b_1 {a_2}^3 + d_1 a_2 + d_1 c_2}{d_1} y + c_2 z + h_2)} \\
&+ k_2 e^{-(a_2 x - \frac{\beta b_1 {a_2}^3 + d_1 a_2 + d_1 c_2}{d_1} y + c_2 z + h_2)} + g_0,
\end{aligned} \tag{21}
$$

and

$$
u_1 = \frac{2{a_2}^2}{f^2}(2k_1 k_2 - {k_1}^2 e^{2\zeta_2} - {k_2}^2 e^{-2\zeta_2} + k_1 f e^{\zeta_2} + k_2 f e^{-\zeta_2}), \tag{22}
$$

$$
\begin{aligned}
v_1 = \frac{-2a_2}{d_1 f^2}&(2k_1 k_2 b_1 {a_2}^3 \beta - {k_1}^2 b_1 {a_2}^3 \beta e^{2\zeta_2} \\
&- {k_2}^2 b_1 {a_2}^3 \beta e^{-2\zeta_2} + k_1 b_1 {a_2}^3 \beta f e^{\zeta_2} + k_2 b_1 {a_2}^3 \beta f e^{-\zeta_2} \\
&+ 2k_1 k_2 d_1 a_2 + 2k_1 k_2 d_1 c_2 - {k_1}^2 d_1 a_2 e^{2\zeta_2} - {k_1}^2 d_1 c_2 e^{2\zeta_2} \\
&- {k_2}^2 d_1 a_2 e^{-2\zeta_2} - {k_2}^2 d_1 c_2 e^{-2\zeta_2} \\
&+ k_1 d_1 a_2 f e^{\zeta_2} + k_1 d_1 c_2 f e^{\zeta_2} + k_2 d_1 a_2 f e^{-\zeta_2} \\
&+ k_2 d_1 c_2 f e^{-\zeta_2} + 2k_1 d_1 b_1 \zeta_1 e^{\zeta_2} - 2k_2 d_1 b_1 \zeta_1 e^{-\zeta_2}),
\end{aligned} \tag{23}
$$

where

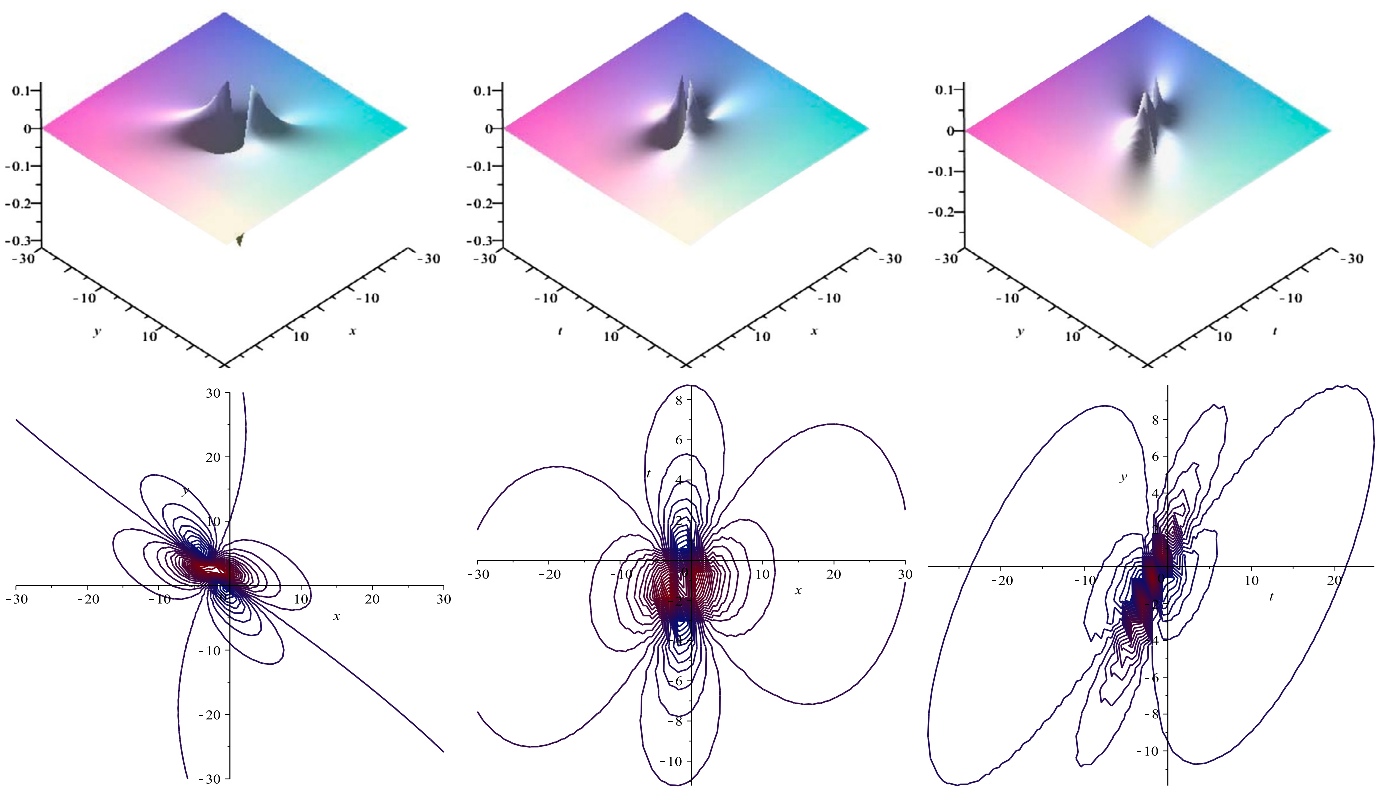

(I) (II) (III)

Fig. 2. The 3-D plots (top) and contour plots (bottom) of v_1 via Eq. (17) at three coordinates: (I) the x_y_v-coordinate by $z=-x$, $t=0$; (II) the x_t_v-coordinate by $z=-x$, $y=0$; (III) the t_y_v-coordinate by $z=-y$, $x=0$; with $a_1=0.2$, $d_1=1$, $h_1=1$, $a_2=0.2$, $b_2=0.2$, $d_2=0.2$, $h_2=1$, $g_0=1$, $\alpha=2$, $\beta=2$.

$$\zeta_1 = b_1 y - b_1 z + d_1 t + h_1,$$
$$\zeta_2 = a_2 x - \frac{\beta b_1 {a_2}^3 + d_1 a_2 + d_1 c_2}{d_1} y + c_2 z + h_2. \tag{24}$$

In addition, we can also obtain the following seven sets of solutions for the parameters $a_i, b_i, c_i, d_i, h_i (i=1,2)$ and $k_i (i=1,2)$:

$$\{a_1 = a_1, b_i = b_i (i=1,2),$$
$$c_1 = -a_1 - b_1, h_i = h_i (i=1,2), a_2 = 0, c_2 = -b_2,$$
$$d_i = d_i (i=1,2), g_0 = g_0, k_1 = k_1,$$
$$\beta = \beta, k_2 = k_2, \alpha = -\frac{\beta b_1}{a_1}\},$$
$$\{a_i = a_i (i=1,2), b_1 = -\frac{a_1 b_2}{a_2},$$
$$c_1 = -\frac{a_1 (a_2 + b_2)}{a_2}, d_i = d_i (i=1,2), b_2 = b_2,$$
$$c_2 = -a_2 - b_2, h_i = h_i (i=1,2), g_0 = g_0, k_1 = k_1,$$
$$\beta = \beta, k_2 = k_2, \alpha = -\frac{\beta b_2}{a_2}\},$$
$$\{a_1 = 0, d_i = d_i (i=1,2), b_1 = 0, c_1 = 0, a_2 = -b_2 - c_2,$$
$$b_2 = b_2, k_1 = k_1,$$
$$\beta = -\frac{\alpha (b_2 + c_2)}{b_2}, c_2 = c_2, h_i = h_i (i=1,2),$$
$$g_0 = g_0, k_2 = k_2, \alpha = \alpha\},$$
$$\{a_1 = 0, b_i = b_i (i=1,2), c_1 = -\frac{b_1 (\beta {a_2}^3 + d_2)}{d_2},$$
$$d_1 = 0, h_i = h_i \ (i=1,2),$$
$$a_2 = a_2, k_1 = k_1, \beta = \beta, c_2 = -a_2 - b_2, d_2 = d_2, g_0 = g_0,$$
$$k_2 = k_2, \alpha = -\frac{\beta b_2}{a_2}\},$$
$$\{a_1 = 0, d_i = d_i (i=1,2), b_1 = 0, c_1 = 0, a_2 = a_2,$$
$$b_2 = -\frac{\alpha a_2}{\beta}, k_1 = k_1,$$
$$c_2 = -\frac{(\beta - \alpha) a_2}{\beta}, h_i = h_i (i=1,2),$$
$$g_0 = {h_1}^2, \beta = \beta, k_2 = k_2, \alpha = \alpha\},$$
$$\{a_1 = 0, b_i = b_i (i=1,2), c_1 = -\frac{b_1 (\beta {a_2}^3 + d_2)}{d_2}, d_1 = 0,$$
$$h_i = h_i (i=1,2), a_2 = a_2,$$
$$k_1 = 0, c_2 = -\frac{\beta {a_2}^3 b_2 + \alpha {a_2}^4 + a_2 d_2 + b_2 d_2}{d_2},$$
$$d_2 = d_2, g_0 = g_0, \beta = \beta, k_2 = k_2, \alpha = \alpha\},$$
$$\{a_1 = 0, b_1 = -\frac{d_1 (a_2 + b_2 + c_2)}{\beta {a_2}^3},$$
$$c_1 = \frac{d_1 (a_2 + b_2 + c_2)}{\beta {a_2}^3}, a_2 = a_2, d_i = d_i (i=1,2), b_2 = b_2,$$
$$h_i = h_i (i=1,2), c_2 = c_2, g_0 = g_0, k_1 = 0, \beta = \beta,$$
$$k_2 = k_2, \alpha = -\frac{\beta {a_2}^3 b_2 + a_2 d_2 + b_2 d_2 + c_2 d_2}{{a_2}^4}\}.$$

These sets of solutions for the parameters generate seven types of solutions $f_i (i=2,3,\ldots,8)$, defined by (19), to the bilinear Eq. (10); and further the resulting seven types of rogue wave type solutions $u_i (i=2,3,\ldots,8)$ and $v_i (i=2,3,\ldots,8)$ to Eq. (2), under the transformation Eq. (5).

The 3-D dynamic graphs of the rogue wave and corresponding density plots are successfully depicted in Fig. 3 and Fig. 4.

Here, a type of X-like rogue wave, which is a mixed solution of a lump wave and two solitary waves, is for the first time found for the $(3+1)$-dimensional GBS equation in Fig. 3 and Fig. 4. At the same time, the energy and the amplitude of the X-like rogue wave achieve the maximum values in the plotted region.

4. Breather lump wave solutions

To search for breather lump wave solutions for Eq. (2), suppose

$$f = \mathrm{e}^{-p_1\zeta_1} + k_1\cos(p_2\zeta_2) + k_2\mathrm{e}^{p_1\zeta_1} + g_0, \tag{25}$$

where $\zeta_i = a_i x + b_i y + c_i z + d_i t + h_i, i = 1, 2,$ and $g_0 > 0$. Here $a_i, b_i, c_i, d_i, h_i (i = 1, 2)$, $p_i (i = 1, 2)$ and $k_i (i = 1, 2)$ are real constants to be calculated. Substituting (25) into bilinear Eq. (10), we reach a set of algebraic equations, and then we can derive $a_i, b_i, c_i, d_i, h_i (i = 1, 2)$, $p_i (i = 1, 2)$ and $k_i (i = 1, 2)$, which can be classified into the following cases.

Case 1.

$$\begin{aligned}
&\{a_1 = a_1, b_1 = b_1, c_1 = -a_1 - b_1, d_1 = d_1, a_2 = a_2,\\
&c_2 = -\frac{a_2(a_1+b_1)}{a_1}, d_2 = d_2,\\
&b_2 = \frac{b_1 a_2}{a_1}, g_0 = g_0, k_1 = k_1, \beta = \beta, k_2 = k_2, p_1 = p_1,\\
&\alpha = -\frac{\beta b_1}{a_1}, p_2 = p_2\}.
\end{aligned}$$

Case 2.

$$\begin{aligned}
&\{a_1 = a_1, b_1 = b_1, c_1 = -a_1 - b_1, d_1 = d_1, a_2 = 0,\\
&c_2 = -\frac{b_2(\beta {a_1}^3 {p_1}^2 + d_1)}{d_1},\\
&b_2 = b_2, d_2 = 0, g_0 = g_0, k_1 = k_1, \beta = \beta, k_2 = k_2,\\
&p_1 = p_1, \alpha = -\frac{\beta b_1}{a_1}, p_2 = p_2\}.
\end{aligned}$$

Case 3.

$$\begin{aligned}
&\{a_1 = 0, b_1 = b_1, c_1 = \frac{b_1(\beta {a_2}^3 {p_2}^2 - d_2)}{d_2}, d_1 = 0,\\
&a_2 = a_2, b_2 = -\frac{\alpha a_2}{\beta}, d_2 = 0,\\
&c_2 = -\frac{a_2(\beta-\alpha)}{\beta}, g_0 = 0, k_1 = k_1,\\
&\beta = \beta, k_2 = k_2, p_1 = p_1, \alpha = \alpha, p_2 = p_2\}.
\end{aligned}$$

Case 4.

$$\begin{aligned}
&\{a_1 = 0, b_1 = b_1, c_1 = \frac{b_1(\beta {a_2}^3 {p_2}^2 - d_2)}{d_2}, d_1 = 0,\\
&a_2 = a_2, c_2 = -a_2 - b_2,\\
&b_2 = b_2, d_2 = d_2, g_0 = g_0, k_1 = k_1, \beta = \beta, k_2 = k_2,\\
&p_1 = p_1, \alpha = -\frac{\beta b_2}{a_2}, p_2 = p_2\}.
\end{aligned}$$

Case 5.

$$\begin{aligned}
&\{a_1 = a_1, b_1 = b_1, c_1 = -\frac{\beta {a_2}^3 b_2 {p_1}^2 + a_1 d_2 + b_1 d_2}{d_2},\\
&d_1 = 0, a_2 = 0, b_2 = b_2,\\
&c_2 = -b_2, d_2 = d_2, g_0 = g_0, k_1 = k_1, \beta = \beta, k_2 = k_2,\\
&p_1 = p_1, \alpha = -\frac{\beta b_1}{a_1}, p_2 = p_2\}.
\end{aligned}$$

Case 6.

$$\begin{aligned}
&\{a_1 = a_1, b_1 = \frac{a_1 b_2}{a_2}, c_1 = -\frac{a_1(a_2+b_2)}{a_2}, d_1 = 0, a_2 = 0,\\
&b_2 = b_2, c_2 = -a_2 - b_2,\\
&d_2 = d_2, g_0 = g_0, k_1 = k_1, \beta = \beta, k_2 = k_2,\\
&p_1 = p_1, \alpha = -\frac{\beta b_2}{a_2}, p_2 = p_2\}.
\end{aligned}$$

Case 7.

$$\begin{aligned}
&\{a_1 = 0, b_1 = b_1, c_1 = -b_1, d_1 = d_1, a_2 = a_2,\\
&c_2 = \frac{\beta b_1 {a_2}^3 {p_2}^2 - d_1 a_2 - d_1 b_2}{d_1},\\
&b_2 = b_2, d_2 = 0, g_0 = g_0, k_1 = k_1, \beta = \beta, k_2 = k_2,\\
&p_1 = p_1, \alpha = -\frac{\beta b_2}{a_2}, p_2 = p_2\}.
\end{aligned}$$

Case 8.

$$\begin{aligned}
&\{a_1 = a_1, b_1 = -\frac{\alpha a_1}{\beta}, c_1 = -\frac{a_1(\beta-\alpha)}{\beta},\\
&d_1 = d_1, c_2 = -\frac{b_2(\beta {a_1}^3 {p_1}^2 + d_1)}{d_1},\\
&a_2 = 0, b_2 = b_2, d_2 = 0, g_0 = 0, k_1 = k_1, \beta = \beta, k_2 = k_2,\\
&p_1 = p_1, \alpha = \alpha, p_2 = p_2\}.
\end{aligned}$$

Case 9.

$$\begin{aligned}
&\{a_1 = a_1, b_1 = -\frac{a_1\alpha}{\beta}, c_1 = -\frac{a_1(\beta^2 {a_1}^2 b_2 {p_1}^2 + \beta d_2 - \alpha d_2)}{d_2\beta},\\
&d_1 = 0, a_2 = 0, b_2 = b_2,\\
&c_2 = -b_2, d_2 = d_2, g_0 = 0, k_1 = k_1, \beta = \beta, k_2 = k_2,\\
&p_1 = p_1, \alpha = \alpha, p_2 = p_2\}.
\end{aligned}$$

Case 10.

$$\begin{aligned}
&\{a_1 = a_1, b_1 = -\frac{\alpha a_1}{\beta}, c_1 = -\frac{a_1(\beta-\alpha)}{\beta}, d_1 = d_1, a_2 = a_2,\\
&b_2 = -\frac{\alpha a_2}{\beta}, d_2 = d_2, c_2 = -\frac{a_2(\beta-\alpha)}{\beta},\\
&g_0 = 0, k_1 = k_1, \beta = \beta, k_2 = k_2, p_1 = p_1, \alpha = \alpha, p_2 = p_2\}.
\end{aligned}$$

Case 1 to Case 10 generate ten types of solutions $f_i (i = 1, 2 \ldots 10)$, defined by (25), to the bilinear Eq. (10); and further the resulting $f_i (i = 1, 2 \ldots 10)$ present ten types of breather lump wave solutions $u_i (i = 1, 2 \ldots 10)$ to Eq. (2), under the transformation $u = 2(\ln f)_{xx}$; and ten types of breather lump wave solutions $v_i (i = 1, 2 \ldots 10)$ to Eq. (2), under the transformation $v = 2(\ln f)_{xy}$. Such as in Case 1, we have

$$\begin{aligned}
f = {} & \mathrm{e}^{-p_1(a_1 x + b_1 y - (a_1+b_1)z + d_1 t + h_1)}\\
& + k_1\cos\left(p_2(a_2 x + \frac{b_1 a_2}{a_1} y - \frac{a_2(a_1+b_1)}{a_1} z + d_2 t + h_2)\right)\\
& + k_2\mathrm{e}^{p_1(a_1 x + b_1 y - (a_1+b_1)z + d_1 t + h_1)} + g_0,
\end{aligned} \tag{26}$$

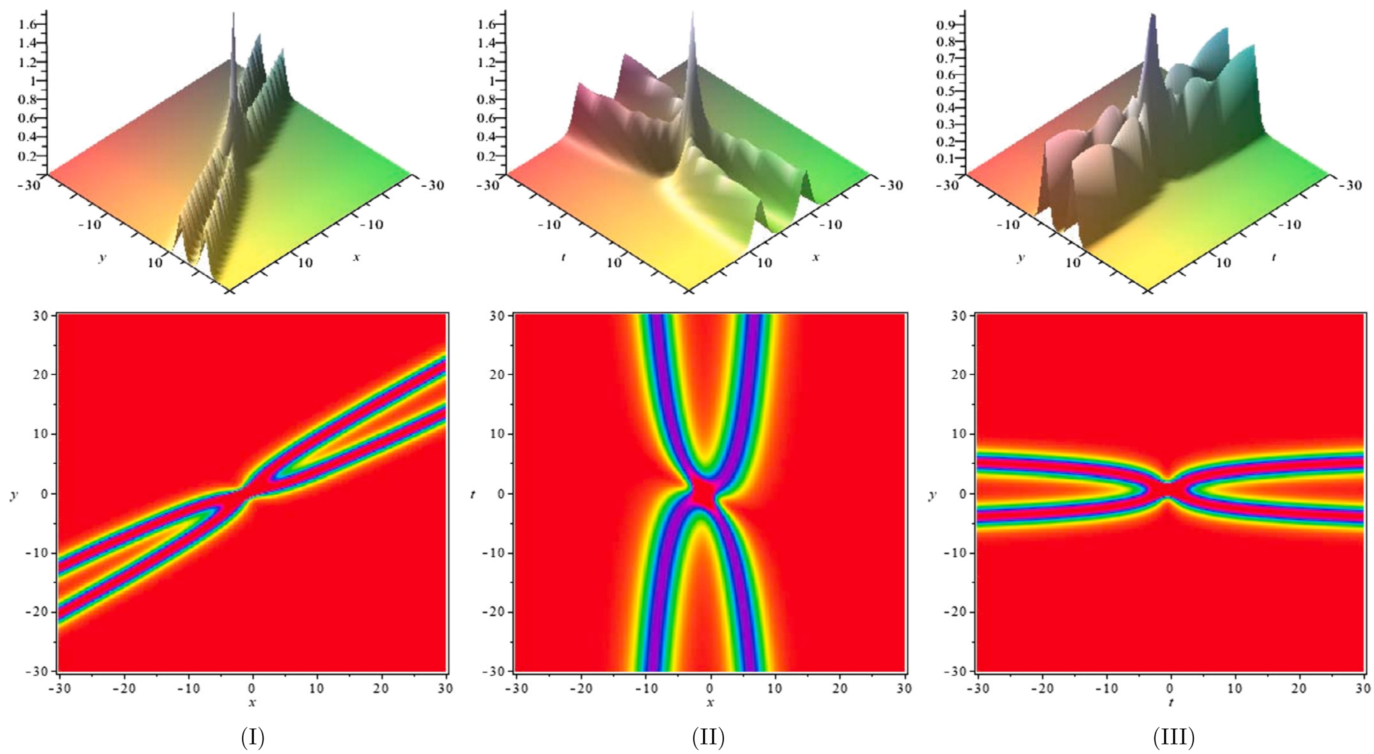

Fig. 3. The 3-D plots (top) and density plots (bottom) of u_1 via Eq. (22) at three coordinates: (I) the x_y_u-coordinate by $z = -x$, $t = 0$; (II) the x_t_u-coordinate by $z = -x$, $y = 0$; (III) the t_y_u-coordinate by $z = y$, $x = 0$; with $b_1 = 1$, $d_1 = 2$, $h_1 = 1$, $a_2 = 1$, $c_2 = 0.1$, $h_2 = 1$, $g_0 = 1$, $k_1 = 4$, $\beta = 1$, $k_2 = 4$.

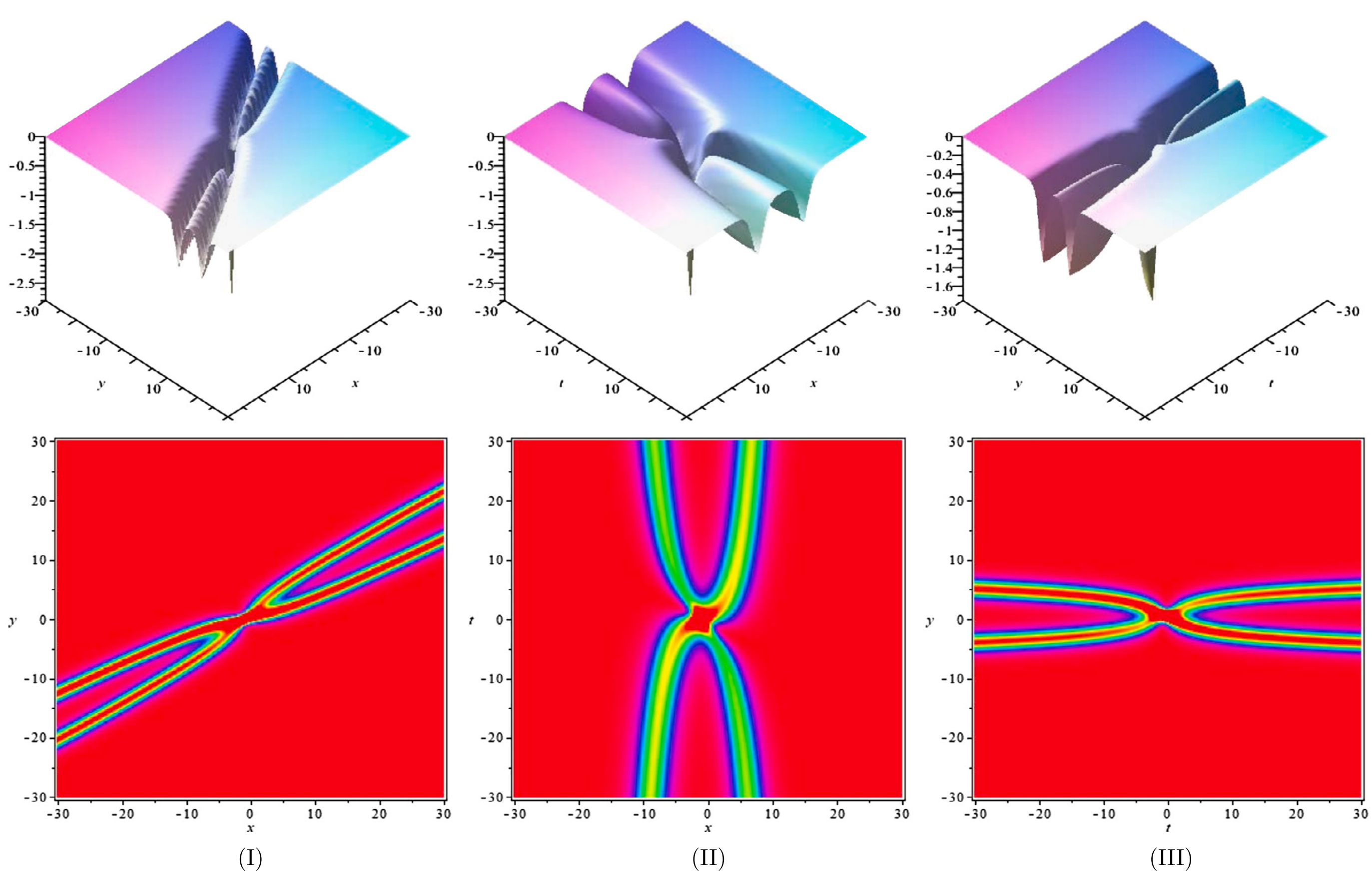

Fig. 4. The 3-D plots (top) and density plots (bottom) of v_1 via Eq. (23) at three coordinates: (I) the x_y_v-coordinate by $z = -x$, $t = 0$; (II) the x_t_v-coordinate by $z = -x$, $y = 0$; (III) the t_y_v-coordinate by $z = y$, $x = 0$; with $b_1 = 1$, $d_1 = 2$, $h_1 = 1$, $a_2 = 1$, $c_2 = 0.1$, $h_2 = 1$, $g_0 = 1$, $k_1 = 4$, $\beta = 1$, $k_2 = 4$.

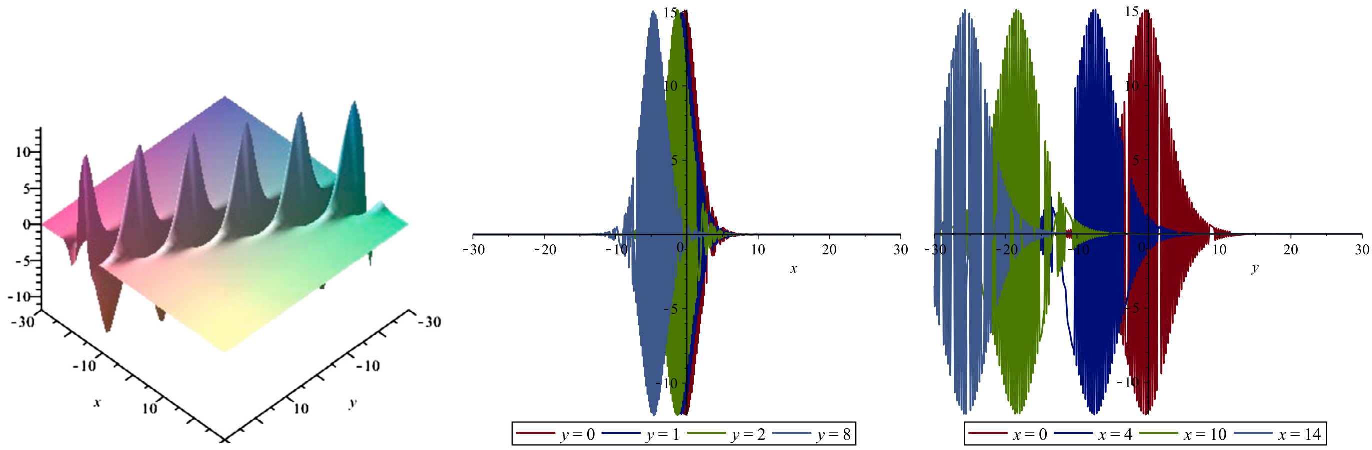

Fig. 5. The 3-D plots and profile plots of u_1 via Eq. (27) at $t=0$ and $z=-x$ with $a_1=0.2$, $b_1=0.5$, $d_1=4$, $h_1=1$, $a_2=8$, $d_2=1$, $h_2=1$, $p_1=1$, $p_2=1$, $k_1=0.2$, $k_2=0.2$, $g_0=1$, $\beta=2$. (For interpretation of the colors in the figure(s), the reader is referred to the web version of this article.)

and

$$\begin{aligned}
u_1 = & \frac{2}{f^2}({k_1}^2{p_2}^2{a_2}^2 f\cos(p_2\zeta_2)^2 - {k_2}^2{p_1}^2{a_1}^2 e^{2p_1\zeta_1} \\
& + 2k_1k_2p_1p_2a_1a_2e^{p_1\zeta_1}\sin(p_2\zeta_2) \\
& - k_1{a_2}^2{p_2}^2 f\cos(p_2\zeta_2) + k_2{p_1}^2{a_1}^2 f e^{p_1\zeta_1} \\
& - 2k_1p_1p_2a_1a_2e^{-p_1\zeta_1}\sin(p_2\zeta_2) \\
& + {p_1}^2{a_1}^2 f e^{-p_1\zeta_1} - {p_1}^2{a_1}^2 e^{-2p_1\zeta_1} \\
& - {k_1}^2{p_2}^2{a_2}^2 + 2k_2{p_1}^2{a_1}^2),
\end{aligned} \tag{27}$$

$$\begin{aligned}
v_1 = & \frac{2b_1}{a_1 f^2}({k_1}^2{p_2}^2{a_2}^2 f\cos(p_2\zeta_2)^2 \\
& - {k_2}^2{p_1}^2{a_1}^2 e^{2p_1\zeta_1} + 2k_1k_2p_1p_2a_1a_2e^{p_1\zeta_1}\sin(p_2\zeta_2) \\
& - k_1{a_2}^2{p_2}^2 f\cos(p_2\zeta_2) + k_2{p_1}^2{a_1}^2 f e^{p_1\zeta_1} \\
& - 2k_1p_1p_2a_1a_2e^{-p_1\zeta_1}\sin(p_2\zeta_2) \\
& + {p_1}^2{a_1}^2 f e^{-p_1\zeta_1} - {p_1}^2{a_1}^2 e^{-2p_1\zeta_1} \\
& - {k_1}^2{p_2}^2{a_2}^2 + 2k_2{p_1}^2{a_1}^2),
\end{aligned} \tag{28}$$

where $a_1 \neq 0$, and the functions ζ_1 and ζ_2 are given as follows:

$$\begin{aligned}
\zeta_1 &= a_1x + b_1y - (a_1+b_1)z + d_1t + h_1, \\
\zeta_2 &= a_2x + \frac{b_1a_2}{a_1}y - \frac{a_2(a_1+b_1)}{a_1}z + d_2t + h_2.
\end{aligned} \tag{29}$$

The 3-D dynamic graphs, corresponding profile plots of the breather lump wave solutions (27) and (28), are successfully depicted in Fig. 5 and Fig. 6.

5. Periodic lump-stripe soliton

In this section, we first propose a type of new interaction solution in terms of a new combination of quadratic function, trigonometric function and exponential function, namely, periodic lump-stripe soliton. Then, we will investigate the interaction between a periodic lump-type soliton and a stripe soliton for Eq. (2), by taking the function f in Eq. (10) in the following form

$$\begin{aligned}
f &= {\zeta_1}^2 + \cos(\zeta_2) + e^{\zeta_3} + g_0, \\
\zeta_i &= a_ix + b_iy + c_iz + d_it + h_i, i = 1, 2, 3,
\end{aligned} \tag{30}$$

where $g_0 > 0$, and $a_i, b_i, c_i, d_i, h_i (i = 1, 2, 3)$ are real constants to be calculated. Substituting (30) into bilinear Eq. (10), we also reach a set of algebraic equations, and then we can derive $a_i, b_i, c_i, d_i, h_i (i = 1, 2, 3)$, which can be classified into the following cases.

Case 1.

$$\begin{aligned}
& a_1 = \frac{b_1a_2}{b_2}, b_i = b_i(i=1,2), c_1 = -\frac{b_1(a_2+b_2)}{b_2}, \\
& d_i = d_i(i=1,2,3), h_i = h_i(i=1,2,3), \\
& a_2 = a_2, c_2 = -a_2 - b_2, a_3 = a_3, b_3 = \frac{b_2a_3}{a_2}, \\
& c_3 = -\frac{a_3(a_2+b_2)}{a_2}, g_0 = g_0, \beta = \beta, \alpha = -\frac{\beta b_2}{a_2},
\end{aligned} \tag{31}$$

where $b_2a_2 \neq 0$. Through the transformation Eq. (5), we get the following solutions to Eq. (2)

$$\begin{aligned}
f = & \left(\frac{b_1a_2}{b_2}x + b_1y - \frac{b_1(a_2+b_2)}{b_2}z + d_1t + h_1\right)^2 \\
& + \cos(a_2x + b_2y - (a_2+b_2)z + d_2t + h_2) \\
& + e^{\left(a_3x + \frac{b_2a_3}{a_2}y - \frac{a_3(a_2+b_2)}{a_2}z + d_3t + h_3\right)} + g_0,
\end{aligned} \tag{32}$$

and

$$\begin{aligned}
u_1 = & \frac{-2}{{b_2}^2 f^2}({a_2}^2{b_2}^2 f\cos(\zeta_2) - {a_3}^2{b_2}^2 f e^{\zeta_3} - {a_2}^2{b_2}^2\cos(\zeta_2)^2 \\
& + {a_3}^2{b_2}^2 e^{2\zeta_3} - 2a_2a_3{b_2}^2 e^{\zeta_3}\sin(\zeta_2) \\
& + 4a_2a_3b_1b_2\zeta_1 e^{\zeta_3} - 4{a_2}^2b_1b_2\zeta_1\sin(\zeta_2) \\
& + 4{a_2}^2{b_1}^2{\zeta_1}^2 - 2{a_2}^2{b_1}^2 f + {a_2}^2{b_2}^2),
\end{aligned} \tag{33}$$

$$\begin{aligned}
v_1 = & \frac{-2}{a_2b_2f^2}({a_2}^2{b_2}^2 f\cos(\zeta_2) \\
& - {a_3}^2{b_2}^2 f e^{\zeta_3} - {a_2}^2{b_2}^2\cos(\zeta_2)^2 \\
& + {a_3}^2{b_2}^2 e^{2\zeta_3} - 2a_2a_3{b_2}^2 e^{\zeta_3}\sin(\zeta_2) \\
& + 4a_2a_3b_1b_2\zeta_1 e^{\zeta_3} - 4{a_2}^2b_1b_2\zeta_1\sin(\zeta_2) \\
& + 4{a_2}^2{b_1}^2{\zeta_1}^2 - 2{a_2}^2{b_1}^2 f + {a_2}^2{b_2}^2),
\end{aligned} \tag{34}$$

where the functions ζ_1, ζ_2 and ζ_3 are given as follows:

$$\begin{aligned}
\zeta_1 &= \frac{b_1a_2}{b_2}x + b_1y - \frac{b_1(a_2+b_2)}{b_2}z + d_1t + h_1, \\
\zeta_2 &= a_2x + b_2y - (a_2+b_2)z + d_2t + h_2, \\
\zeta_3 &= a_3x + \frac{b_2a_3}{a_2}y - \frac{a_3(a_2+b_2)}{a_2}z + d_3t + h_3.
\end{aligned} \tag{35}$$

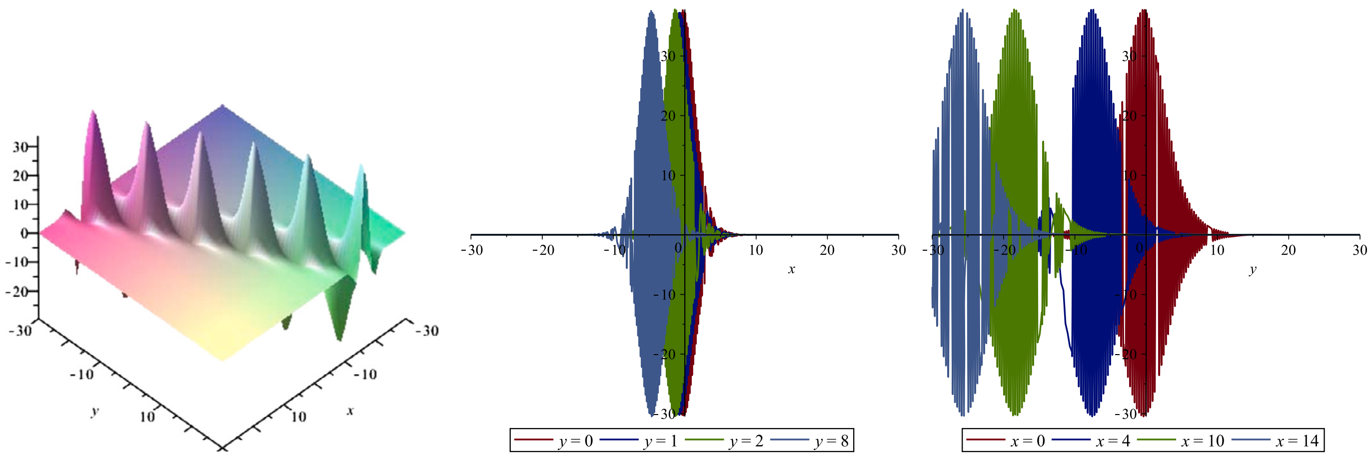

Fig. 6. The 3-D plots and profile plots of v_1 via Eq. (28) at $t=0$ and $z=-x$ with $a_1=0.2$, $b_1=0.5$, $d_1=4$, $h_1=1$, $a_2=8$, $d_2=1$, $h_2=1$, $p_1=1$, $p_2=1$, $k_1=0.2$, $k_2=0.2$, $g_0=1$, $\beta=2$.

Case 2.

$$\{a_1=\frac{b_1a_3}{b_3}, b_1=b_1, c_1=-\frac{b_1(a_3+b_3)}{b_3},$$
$$d_i=d_i(i=1,2,3), a_2=0, b_2=0, \beta=\beta,$$
$$\alpha=-\frac{\beta b_3}{a_3}, c_2=0, h_i=h_i(i=1,2,3),$$
$$a_3=a_3, b_3=b_3, c_3=-a_3-b_3, g_0=g_0\}.$$

Case 3.

$$\{a_1=0, b_i=b_i(i=1,2), c_1=-b_1, d_1=d_1,$$
$$h_i=h_i(i=1,2,3), a_2=a_2, \beta=\beta, g_0=g_0,$$
$$\alpha=-\frac{\beta b_2}{a_2}, c_2=\frac{\beta b_1a_2{}^3-d_1a_2-d_1b_2}{d_1}, d_2=0,$$
$$a_3=0, b_3=-c_3, c_3=c_3, d_3=-\frac{d_1c_3}{b_1}\}.$$

Case 4.

$$\{a_1=\frac{\beta b_1}{-\alpha}, b_1=b_1, c_1=\frac{(\beta-\alpha)b_1}{\alpha}, d_i=d_i(i=1,2,3),$$
$$h_1=0, a_2=a_2, b_2=\frac{\alpha a_2}{-\beta}, \beta=\beta,$$
$$\alpha=\alpha, g_0=g_0, c_2=\frac{(\beta-\alpha)a_2}{-\beta}, h_i=h_i(i=2,3),$$
$$a_3=a_3, b_3=\frac{\alpha a_3}{-\beta}, c_3=\frac{(\beta-\alpha)a_3}{-\beta}\}.$$

Case 5.

$$\{a_1=0, b_1=b_1, c_1=\frac{(\beta a_3{}^3+d_3)b_1}{-d_3}, d_1=0,$$
$$h_1=0, a_2=a_2, b_2=\frac{\alpha a_2}{-\beta}, \beta=\beta,$$
$$\alpha=\alpha, g_0=g_0,$$
$$c_2=\frac{(\beta-\alpha)a_2}{-\beta}, d_2=\frac{a_2{}^3d_3}{-a_3{}^3}, h_2=h_2,$$
$$a_3=a_3, b_3=\frac{\alpha a_3}{-\beta}, c_3=\frac{(\beta-\alpha)a_3}{-\beta}, d_3=d_3, h_3=h_3\}.$$

Case 6.

$$\{a_1=\frac{b_1a_3}{b_3}, b_1=b_1, c_1=\frac{b_1(a_3+b_3)}{-b_3}, d_1=d_1,$$
$$h_1=0, a_2=a_2, b_2=\frac{a_2b_3}{a_3}, \beta=\beta, \alpha=\frac{\beta b_3}{-a_3},$$
$$c_2=\frac{a_2(a_3+b_3)}{-a_3}, d_2=d_2, a_3=a_3,$$
$$h_2=h_2, b_3=b_3, h_3=h_3, c_3=-a_3-b_3, d_3=0, g_0=g_0\}.$$

Case 7.

$$\{a_1=a_1, b_1=\frac{\alpha a_1}{-\beta}, c_1=\frac{(\beta-\alpha)a_1}{\beta}, d_1=0,$$
$$a_2=a_2, b_2=\frac{\alpha a_2}{-\beta}, \beta=\beta, h_i=h_i(i=1,2,3),$$
$$c_2=\frac{(\beta^2a_2{}^2b_3-\beta d_3+\alpha d_3)a_2}{-\beta d_3}, d_2=0,$$
$$a_3=0, c_3=-b_3, b_3=b_3, \alpha=\alpha, d_3=d_3, g_0=g_0\}.$$

Case 8.

$$\{a_1=0, b_1=b_1, c_1=-b_1, d_1=d_1, h_1=h_1,$$
$$a_2=0, b_2=\frac{b_1d_2}{d_1}, \beta=\beta,$$
$$\alpha=\frac{\beta(\beta b_1a_3{}^3+b_1d_3+d_1a_3+d_1c_3)}{d_1a_3}, c_2=-\frac{b_1d_2}{d_1},$$
$$d_2=d_2, h_2=h_2, a_3=a_3,$$
$$b_3=-\frac{\beta b_1a_3{}^3+d_1a_3+d_1c_3}{d_1}, c_3=c_3,$$
$$d_3=d_3, h_3=h_3, g_0=g_0\}.$$

Case 2 to Case 8 generate seven types of solutions $f_i(i=2,3\ldots8)$, defined by (30), to the bilinear Eq. (10); and further the resulting present seven types of periodic lump-stripe solitons $u_i(i=2,3\ldots8)$ and $v_i(i=2,3\ldots8)$ to Eq. (2), under the transformation Eq. (5).

The 3-D dynamic graphs of the periodic lump-stripe soliton v_1, and corresponding density plots are successfully depicted in Fig. 7. We can see the mutual reaction of the lump-type waves, cosine function waves and the exponential function waves. In addition, Fig. 8 and Fig. 9 show 3-D and density evolution behaviors of u_1, by setting $z=-x$ and picking different values for t, where we

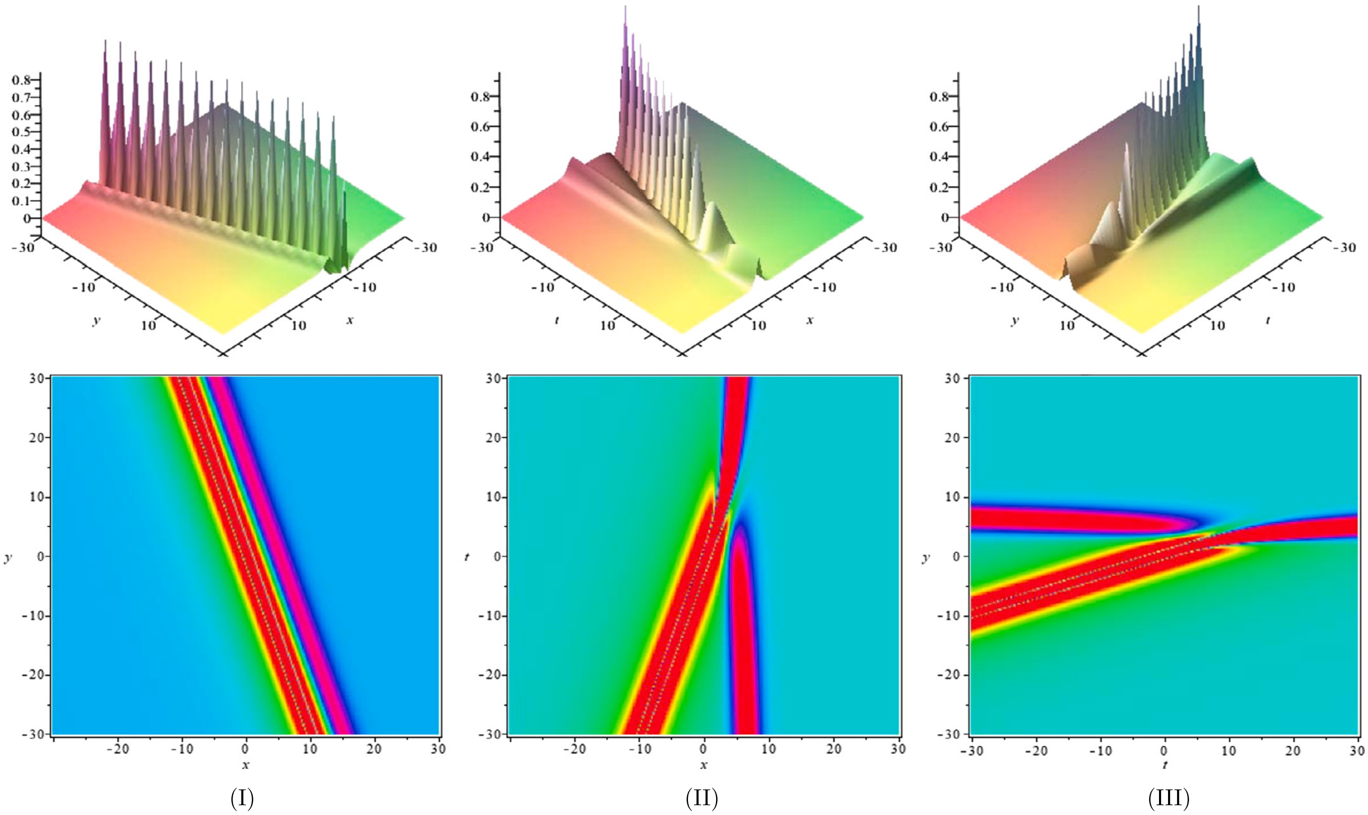

Fig. 7. The 3-D plots and density plots of v_1 via Eq. (34) at three coordinates: (I) the x_y_v-coordinate by $z=-x$, $t=0$; (II) the x_t_v-coordinate by $z=-x$, $y=0$; (III) the t_y_v-coordinate by $z=-y$, $x=0$; with $b_1=-1$, $d_1=1$, $h_1=1$, $a_2=0.1$, $b_2=0.1$, $d_2=0$, $h_2=1$, $a_3=0.5$, $d_3=0$, $h_3=-2$, $g_0=4$, $\beta=2$.

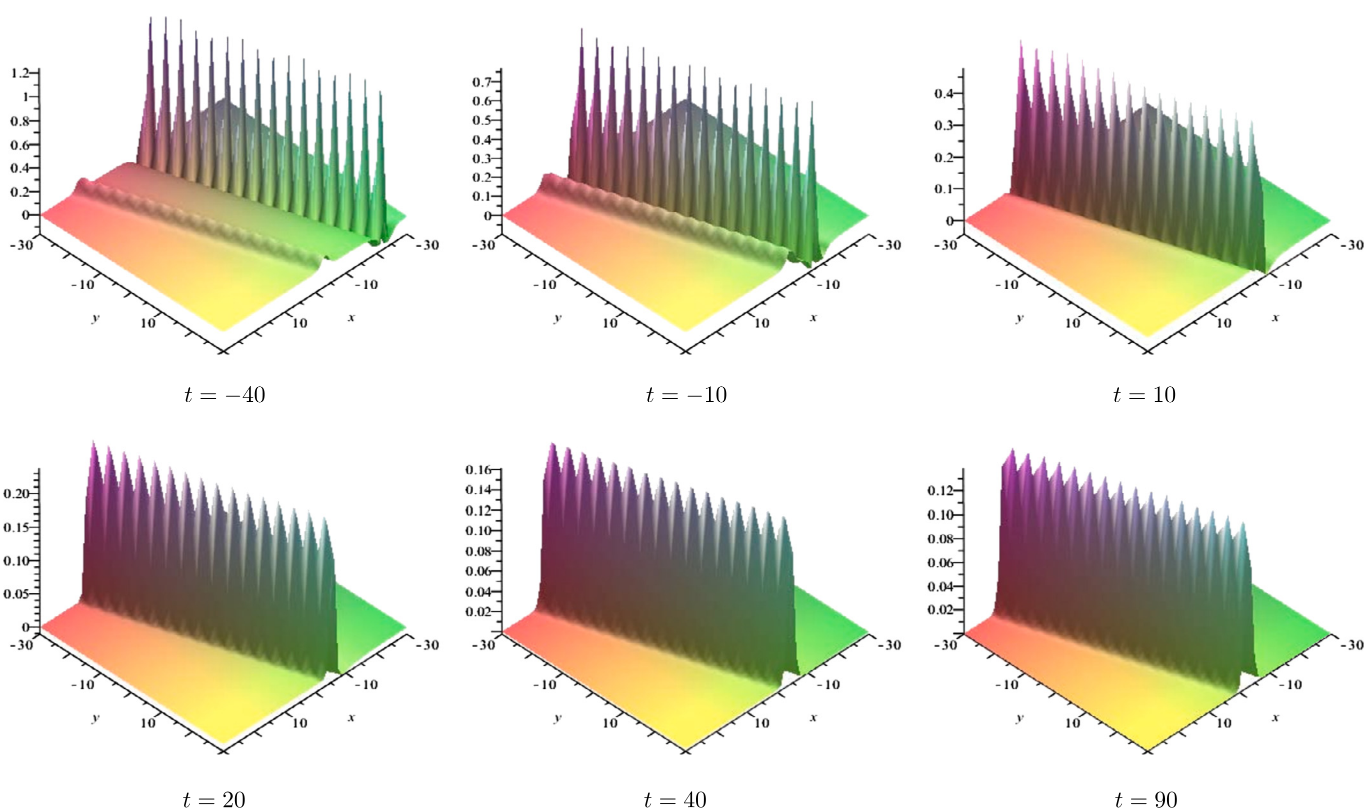

Fig. 8. The 3-D evolution plots of u_1 via Eq. (33) at $t=-40$, $t=-10$, $t=10$, $t=20$, $t=40$ and $t=90$ with $z=-x$, $b_1=-1$, $d_1=1$, $h_1=1$, $a_2=0.1$, $b_2=0.1$, $d_2=0$, $h_2=1$, $a_3=0.5$, $d_3=0$, $h_3=-2$, $g_0=4$, $\beta=2$.

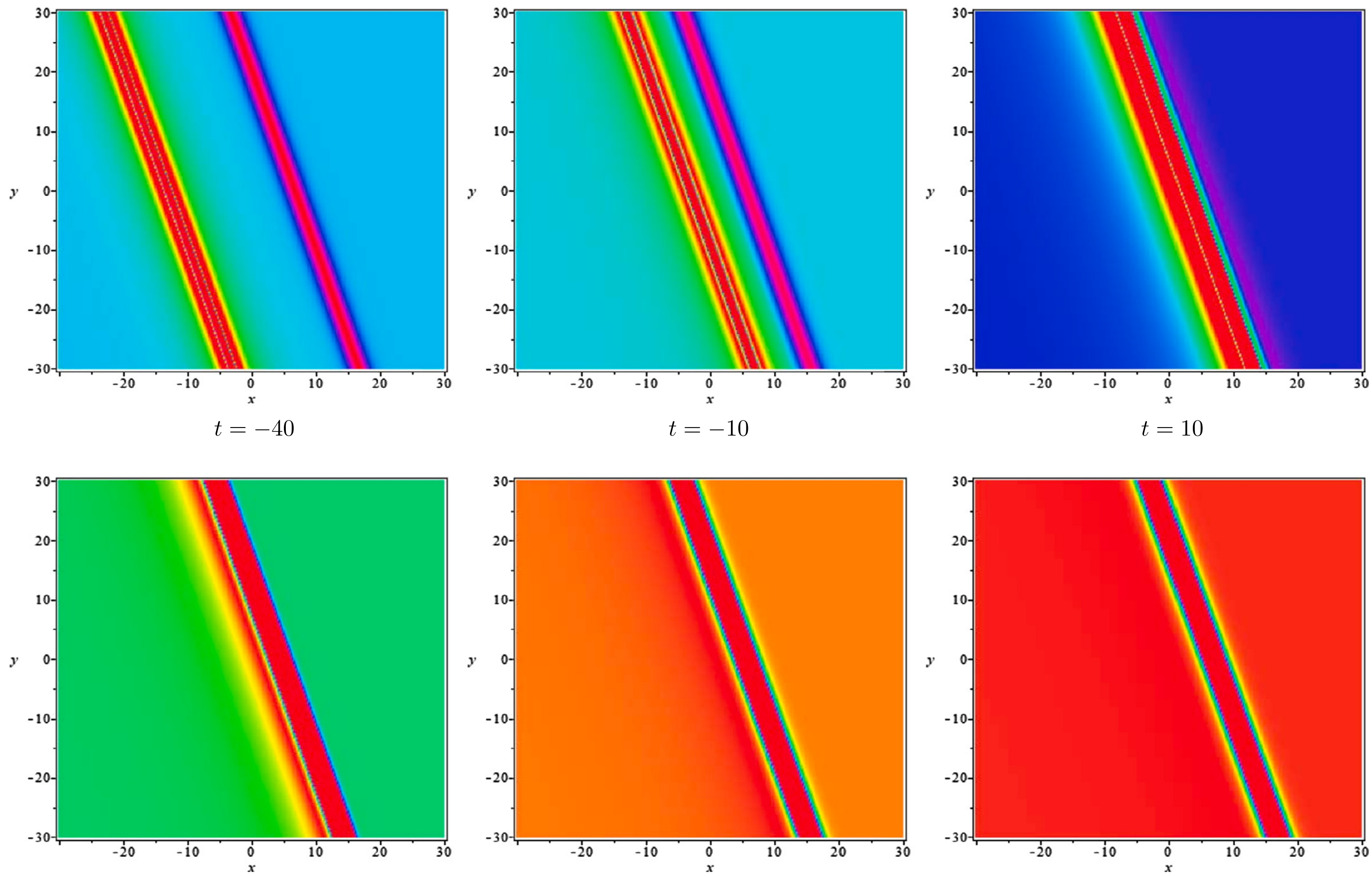

Fig. 9. The density evolution plots of u_1 via Eq. (33) at $t=-40$, $t=-10$, $t=10$, $t=20$, $t=40$ and $t=90$ with $z=-x$, $b_1=-1$, $d_1=1$, $h_1=1$, $a_2=0.1$, $b_2=0.1$, $d_2=0$, $h_2=1$, $a_3=0.5$, $d_3=0$, $h_3=-2$, $g_0=4$, $\beta=2$.

change the coordinate of the periodic lump-type soliton to make it collide with stripe soliton.

The periodic lump-type soliton and a stripe soliton begin appearing at $t=-40$ in Fig. 8 and Fig. 9. The amplitude of the stripe soliton starts to increase as the periodic lump-type soliton approaches the stripe soliton. The periodic lump-type soliton begins colliding with the stripe soliton when $t=10$. Finally, the periodic lump-type soliton completely decays and is swallowed by the stripe soliton when $t=90$ in Fig. 8 and Fig. 9, where the energy and the amplitude of the periodic lump-stripe soliton have the maximum values. We see that periodic lump-stripe soliton is completely non-elastic, $u(x,y,z,t)$ and $v(x,y,z,t)$ are mixed solitary waves of quadratic function, trigonometric function and exponential function, and they decays both exponentially and algebraically. This interaction phenomena is similar to the fusion and fission for soliton solutions.

6. Summary and discussions

In this paper, we obtained a bilinear form for Eq. (2), through using a Hirota direct method. Then, abundant new lump-type solutions, rogue wave type solutions, breather lump wave solutions and periodic lump-stripe solitons were constructed, by utilizing the Hirota bilinear form. It is expected that those new solutions would be helpful in better understanding the $(3+1)$-dimensional GBS equation. We presented lump-type solitons and their dynamic characteristics in Fig. 1 and Fig. 2. The 3-D dynamics characteristics and density plots of the rogue wave, breather lump waves and periodic lump-stripe solitons were depicted in Figs. 3 and 4; and Figs. 5 and 6; and Fig. 7; respectively. In addition, we also investigated another type of X-like rogue wave, by taking the function f in Eq. (10) in the following form

$$f=\zeta_1{}^2+\zeta_2{}^2+\cosh(\zeta_3)+g_0,$$
$$\zeta_i=a_ix+b_iy+c_iz+d_it+h_i,\ (i=1,2,3). \tag{36}$$

For an example, for a group of parameters:

$$a_i=a_i(i=1,2,3),\ b_1=\frac{b_3(a_1{}^2+a_2{}^2)-a_2b_2a_3}{a_1a_3},$$
$$c_1=-\frac{a_1{}^2(a_3+b_3)+a_2{}^2b_3-a_2b_2a_3}{a_1a_3},$$
$$d_1=d_1,\ h_i=h_i(i=1,2,3),\ b_2=b_2,\ c_2=-a_2-b_2,$$
$$d_2=-\frac{a_1d_1}{a_2},\ b_3=b_3,$$
$$c_3=-\frac{\beta a_2{}^2a_3{}^2b_3-\beta a_2b_2a_3{}^2+a_1d_1(a_3+b_3)}{a_1d_1},$$
$$d_3=0,\ g_0=g_0,\ \beta=\beta,\ \alpha=-\frac{\beta b_3}{a_3},$$

where $a_1d_1a_2a_3\neq 0$. Then, we can present rogue wave type solutions for Eq. (2), under the transformation Eq. (5). The graphs of corresponding u and v are given in Fig. 10.

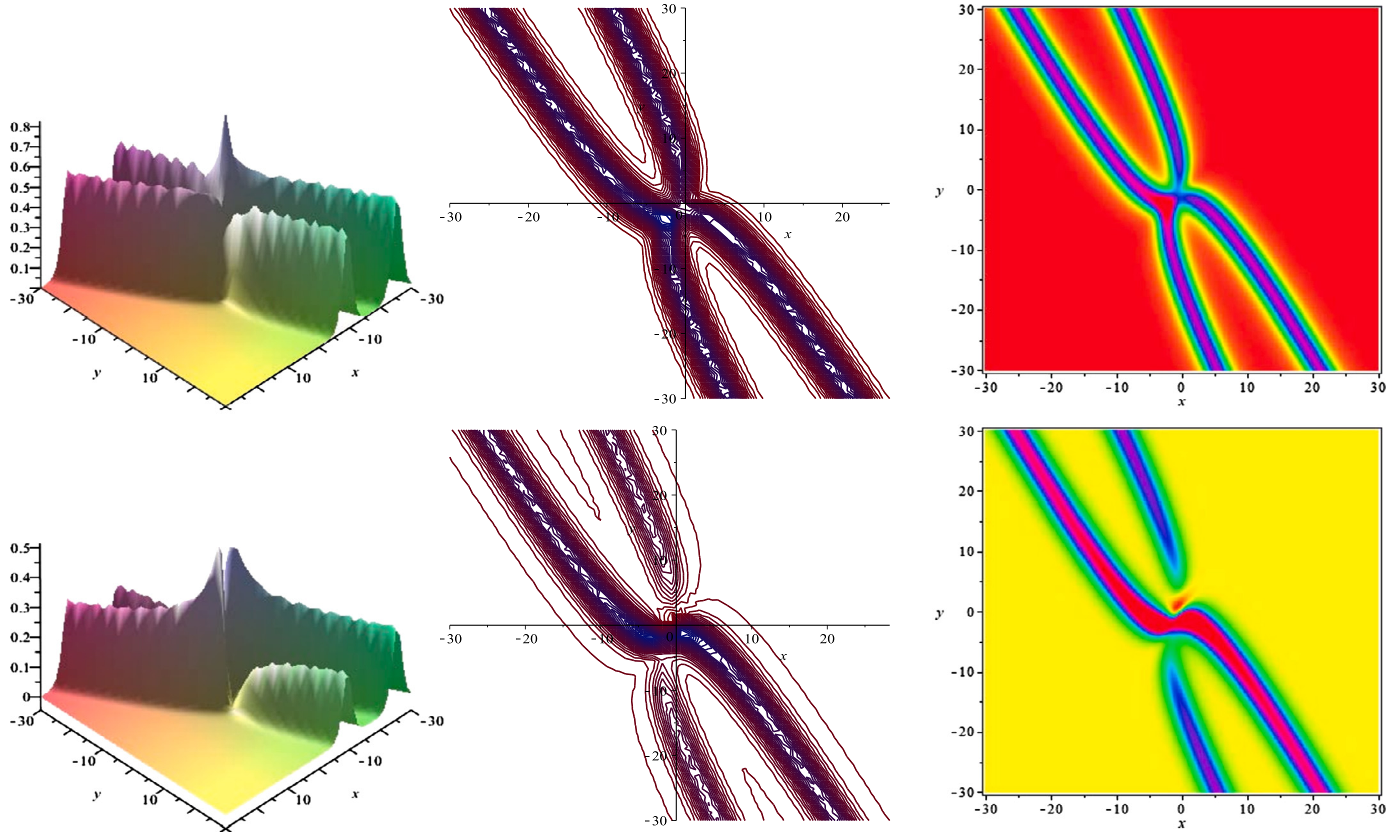

Fig. 10. Plots of the second type of rogue wave solutions u (top) and v (bottom) at $t = 0$ with $z = x$, $a_1 = 0.2$, $d_1 = 0.2$, $h_1 = 1$, $a_2 = 0.2$, $b_2 = -0.5$, $h_2 = 1$, $a_3 = 1$, $b_3 = 0.5$, $h_3 = 2$, $g_0 = 1$, $\beta = -0.5$.

The 3-D and density evolution behaviors of the periodic lump-stripe solitons were depicted in Fig. 8 and Fig. 9. We changed the coordinate of the periodic lump-type soliton to make it collide with the stripe soliton, through setting $t = -40$, $t = -10$, $t = 10$, $t = 20$, $t = 40$ and $t = 90$. Moreover, we observed that the periodic lump-type soliton is swallowed by the stripe soliton. It should be particularly interesting to note that, by taking $p = 3$, $p = 5$ and $p = 7$, the bilinear Eq. (10) can take one of the following generalized bilinear forms:

$$\begin{aligned} &\big(D_{3,x}D_{3,t} + D_{3,y}D_{3,t} + D_{3,z}D_{3,t} + \alpha D_{3,x}^4 \\ &\quad + \beta D_{3,x}^3 D_{3,y}\big) f \cdot f = 0, \qquad (37) \\ &\big(D_{5,x}D_{5,t} + D_{5,y}D_{5,t} + D_{5,z}D_{5,t} + \alpha D_{5,x}^4 \\ &\quad + \beta D_{5,x}^3 D_{5,y}\big) f \cdot f = 0, \qquad (38) \\ &\big(D_{7,x}D_{7,t} + D_{7,y}D_{7,t} + D_{7,z}D_{7,t} + \alpha D_{7,x}^4 \\ &+ \beta D_{7,x}^3 D_{7,y}\big) f \cdot f = 0, \qquad (39) \end{aligned}$$

whose lump-type solutions, rogue wave type solutions, breather lump wave solutions and periodic lump-stripe solitons can be similarly generated. Our future study will focus on implementing the Hirota bilinear method to present exact solutions of higher order bilinear equations and extending the Hirota bilinear method to a larger research field.

Declaration of competing interest

The authors declare that they have no known competing financial interests or personal relationships that could have appeared to influence the work reported in this paper.

Acknowledgements

The authors would like to thank the editors and reviewers for their suggestions and comments.

Funding. The authors are supported by the National Natural Science Foundation of China (Grants No. 61572095, 61877007).

References

[1] W.X. Ma, Lump solutions to the Kadomtsev–Petviashvili equation, Phys. Lett. A 379 (2015) 1975–1978.
[2] S. Manukure, Y. Zhou, W.X. Ma, Lump solutions to a $(2+1)$-dimensional extended KP equation, Comput. Math. Appl. 75 (2018) 2414–2419.
[3] B. Ren, W.X. Ma, J. Yu, Characteristics and interactions of solitary and lump waves of a $(2+1)$-dimensional coupled nonlinear partial differential equation, Nonlinear Dyn. 96 (2019) 717–727.
[4] W.X. Ma, Y. Zhou, Lump solutions to nonlinear partial differential equations via Hirota bilinear forms, J. Differ. Equ. 264 (2018) 2633–2659.
[5] J.Y. Yang, W.X. Ma, Abundant lump-type solutions of the Jimbo–Miwa equation in $(3+1)$-dimensions, Comput. Math. Appl. 73 (2017) 220–225.
[6] W.X. Ma, Abundant lumps and their interaction solutions of $(3+1)$-dimensional linear PDEs, J. Geom. Phys. 133 (2018) 10–16.
[7] W.X. Ma, Lump and interaction solutions of linear PDEs in $(3+1)$-dimensions, East Asian J. Appl. Math. 9 (2019) 185–194.
[8] M. Wang, B. Tian, Y. Sun, H.M. Yin, Z. Zhang, Mixed lump-stripe, bright rogue wave-stripe, dark rogue wavestripe and dark rogue wave solutions of a generalized Kadomtsev–Petviashvili equation in fluid mechanics, Chin. J. Phys. 60 (2019) 440–449.
[9] X.G. Geng, Y.L. Ma, N-soliton solution and its Wronskian form of a $(3+1)$-dimensional nonlinear evolution equation, Phys. Lett. A 369 (2007) 285–289.
[10] A. Majid Wazwaz, Multiple soliton solutions for the Bogoyavlenskii's generalized breaking soliton equations and its extension form, Appl. Math. Comput. 217 (2010) 4282–4288.
[11] Y. Zhou, S. Manukure, W.X. Ma, Lump and lump-soliton solutions to the Hirota–Satsuma–Ito equation, Commun. Nonlinear Sci. Numer. Simul. 68 (2019) 56–62.
[12] C.H. He, Y.N. Tang, W.X. Ma, J.L. Ma, Interaction phenomena between a lump and other multi-solitons for the $(2+1)$-dimensional BLMP and Ito equations, Nonlinear Dyn. 95 (2019) 29–42.

[13] Y. Zhang, Y.P. Liu, X.Y. Tang, M-lump and interactive solutions to a $(3+1)$-dimensional nonlinear system, Nonlinear Dyn. 93 (2018) 2533–2541.
[14] Y. Zhang, Y.P. Liu, X.Y. Tang, M-lump solutions to a $(3+1)$-dimensional nonlinear evolution equation, Comput. Math. Appl. 76 (2018) 592–601.
[15] Z.L. Zhao, L.C. He, Multiple lump solutions of the $(3+1)$-dimensional potential Yu–Toda–Sasa–Fukuyama equation, Appl. Math. Lett. 95 (2019) 114–121.
[16] B. Ren, W.X. Ma, Rational solutions and their interaction solutions of the $(2+1)$-dimensional modified dispersive water wave equation, Comput. Math. Appl. 77 (2019) 2086–2095.
[17] J.J. Xie, X. Yang, Rogue waves, breather waves and solitary waves for a $(3+1)$-dimensional nonlinear evolution equation, Appl. Math. Lett. 97 (2019) 6–13.
[18] Y.Q. Liu, X.Y. Wen, Novel interaction phenomena of localized waves in the generalized $(3+1)$-dimensional KP equation, Comput. Math. Appl. 78 (2019) 1–19.
[19] Y.Q. Yuan, B. Tian, L. Liu, X.Y. Wu, Y. Sun, Solitons for the $(2+1)$-dimensional Konopelchenko–Dubrovsky equations, J. Math. Anal. Appl. 460 (2018) 476–486.
[20] Z. Du, B. Tian, H.P. Chai, Y. Sun, X.H. Zhao, Rogue waves for the coupled variable-coefficient fourth-order nonlinear Schrödinger equations in an inhomogeneous optical fiber, Chaos Solitons Fractals 109 (2018) 90–98.
[21] X.Y. Gao, Mathematical view with observational/experimental consideration on certain $(2+1)$-dimensional waves in the cosmic/laboratory dusty plasmas, Appl. Math. Lett. 91 (2019) 165–172.
[22] X.H. Zhao, B. Tian, X.Y. Xie, X.Y. Wu, Y. Sun, Y.J. Guo, Solitons, Bäcklund transformation and Lax pair for a $(2+1)$-dimensional Davey-Stewartson system on surface waves of finite depth, Waves Random Complex Media 28 (2018) 356–366.
[23] S.S. Chen, B. Tian, L. Liu, Y.Q. Yuan, C.R. Zhang, Conservation laws, binary Darboux transformations and solitons for a higher-order nonlinear Schrödinger system, Chaos Solitons Fractals 118 (2019) 337–346.
[24] X.Y. Gao, Looking at a nonlinear inhomogeneous optical fiber through the generalized higher-order variable-coefficient Hirota equation, Appl. Math. Lett. 73 (2017) 143–149.
[25] Z. Wang, Y.p. Qin, L. Zou, Quasi-periodic solutions and asymptotic properties for the nonlocal Boussinesq equation, Chin. Phys. B 26 (2017) 050504.
[26] Y.L. Ma, B.Q. Li, Interactions between soliton and rogue wave for a $(2+1)$-dimensional generalized breaking soliton system: hidden rogue wave and hidden soliton, Comput. Math. Appl. 78 (2019) 827–839.
[27] X.W. Yan, S.F. Tian, M.J. Dong, L. Zhou, T.T. Zhang, Characteristics of solitary wave, homoclinic breather wave and rogue wave solutions in a $(2+1)$-dimensional generalized breaking soliton equation, Comput. Math. Appl. 76 (2018) 179–186.
[28] M.S. Osman, On multi-soliton solutions for the $(2+1)$-dimensional breaking soliton equation with variable coefficients in a graded-index waveguide, Comput. Math. Appl. 75 (2018) 1–6.
[29] O.A. Ilhan, J. Manafian, Periodic type and periodic cross-kink wave solutions to the $(2+1)$-dimensional breaking soliton equation arising in fluid dynamics, Mod. Phys. Lett. B 33 (2019) 1950277.
[30] H.Q. Sun, A.H. Chen, Lump and lump-kink solutions of the $(3+1)$-dimensional Jimbo–Miwa and two extended Jimbo–Miwa equations, Appl. Math. Lett. 68 (2017) 55–61.
[31] J.g. Liu, X.J. Yang, M.H. Cheng, Y.Y. Feng, Y.D. Wang, Abound rogue wave type solutions to the extended $(3+1)$-dimensional Jimbo–Miwa equation, Comput. Math. Appl. 78 (2019) 1947–1959.